Type of the Paper (Article)

Preparation and Tribological Behaviours of Lubrication Enhanced PEEK Composites

Yan Yutao[1,*], Jiang Cheng[1], Huo Yuqiu[2,*], Li Chaofeng[1]

[1] School of Mechanical Engineering and Automation, Northeastern University, Shenyang, 11089, China ; ytyan@mail.neu.edu.cn
[2] Department of chemistry, College of Science, Northeastern University, Shenyang, 11089, China ; huoyuqiu@mail.neu.edu.cn
* Correspondence: ytyan@mail.neu.edu.cn, huoyuqiu@mail.neu.edu.cn;

Abstract: Poly-ether-ether ketone (PEEK) is a great potential thermoplastic in industry and medical treatment and health. In this work, the PEEK/GO and PEEK/MoS_2 composites were prepared by a novel hot isostatic pressing method. The addition of GO alters the tribological behaviours mechanism, fatigue wear mechanism is predominant to PEEK/GO composites. However, the combination of abrasive and adhesive wear mechanisms is observed for PEEK/MoS_2 composites and PEEK. The reason is the hardness and tensile strength of composites are increased with the appropriate addition of GO. The response time to stable friction state of PEEK/GO and PEEK/MoS_2 composites reduces in compared with PEEK, which conduce to shorten running-in time, reduce energy consumption and improve the tribological performances of composites. The addition of GO and MoS_2 can effectively decrease the friction coefficient and wear rate, and the optimal content of GO and MoS_2 was 0.7 wt.% and 15 wt.%, respectively. The results indicate that PEEK/GO and PEEK/MoS_2 are impressive composites that possess super tribological properties.

Keywords: poly-ether-ether ketone; graphene oxide (GO); MoS_2; tribological behaviours; mechanism

1. Introduction

Poly-ether-ether ketone (PEEK), first synthesized by Bonner in 1962, is an excellent aromatic semi-crystalline thermoplastic engineering plastic with great mechanical properties [1,2], excellent chemical corrosion resistance, thermal stability and suitable tribological characteristics [3], high radiation resistance [4], good machinability and electrical properties [5]. PEEK is widely used in the fields of aerospace, nuclear industries, machinery, transportation, electronics, energy, marine, medical treatment and health etc. [6,7]. In most cases, PEEK composites are selected in non-lubricated applications, which are also required to withstand high loads and long working hours. However, the PEEK exhibits relatively high friction coefficient and low wear resistance due to its stronger adhesion to counterpart materials, which makes difficult to meet the operating requirements under harsh dry sliding contacts conditions [1,6,8]. The properties of PEEK composites are affected by the preparation methods, the conventional method including injection moulding [9,10], compression moulding [11,12] and extrusion[13,14].

Graphene was first obtained from graphite by Geim et al. at Manchester University in 2004 [15]. It possesses outstanding conductive capacity [16], extraordinary thermal conductivity [17], outstanding mechanical properties [16] and excellent tribological properties [17]. Puértolas et al. [3] has prepared the graphene nanoplatelet/PEEK composites by solvent-free melt-blending and injection molding, and studied its thermal characterizations, mechanical properties and tribological

behaviours. The results indicate that microstructural parameters and thermal conductivity of the composites are not modified. However, there is an increase in the modulus and hardness, as well as a decrease in the toughness, friction coefficient and wear factor owning to the addition of graphene nanoplate. Yetgin [18] has carried out the research on the friction and wear properties of polypropylene (PP) composites with graphene oxides (GO) prepared by a twin-screw extruder followed by injection moulding. It is found that the friction coefficient and wear rate of PP nanocomposites are increased with increase of applied loads and sliding speeds, but lower than that of unfilled PP. Interesting, the addition of GO increases the tensile strength, but has little effect on hardness. It was reported that the addition of graphene clearly enhanced the friction reduction and wear resistance properties of polyimide by Roy [19]. A number of research results show that the addition of graphene can obviously enhance the friction reduction and wear resistance of polymers, such as PEEK [3,6,9], polytetrafluoroethylene (PTFE) [20], polyphenylene sulphide (PPS) [21], acrylonitrile butadiene rubbers (NBRs) [22], phenolic [23], bismaleimide (BMI) [7], polyamide (PA) [16], ultra-high molecular weight polyethylene (UHMWPE) [24] and so on.

It is well known that molybdenum disulfide (MoS_2) is one of super solid lubricants and friction modifiers owning to its unique layered structure with the weak van der Waals interaction between layers [7,25]. Many research results indicate that the addition of MoS_2 in lubricating oils or greases has greater effects on a friction reduction, wear resistance and prolonged life expectancy for the friction system [26-28]. Tang et al. [29] has synthesized the MoS_2 flower-like microspheres via Pluronic F-127 assisted hydrothermal method and studied its tribological properties as an additive in liquid paraffin. On the other hand, MoS_2 has also been studied as one of the solid lubricant fillers to improve the self-lubricating properties of polymers matrix in dry sliding conditions. Chen et al. [12] has investigated the characteristics of polyimide composite which composes of carbon fiber and MoS_2 obtained by a one-step hydrothermal method. The friction and wear properties as well as the hardness and thermal stability of polyimide composite are improved. Zalaznik et al. [25] has studied the thermal, mechanical and tribological properties of PEEK/MoS_2 composites. The results exhibit the content of MoS_2 had a certain effect on the thermal, mechanical and tribological properties. It is reported that the tribological properties of high-density polyethylene/MoS_2 composite is related to crystallinity and thermo-mechanical properties [30]. The composites with lower damping factors and better crystallinity show better tribological properties. The composites with different content of MoS_2 exhibit the different wear mechanisms due to the enhancement of heat dissipation performance of MoS_2. The low content is mainly the combination of adhesive wear and abrasive wear, while the high content shows a certain fatigue wear characteristics.

Based on the above investigations, the PEEK composites with different content of GO and MoS_2 are obtained via a novel hot isostatic pressing method in this paper. The mechanical properties and tribological behaviours are studied. In particular, the response time to a stable friction state of composites is investigated. The mechanism of friction and wear is investigated by SEM and three dimensional optical morphologies.

2. Materials and Methods

2.1 Materials

The PEEK was provided in a powder form by Jilin Joinature Polymer Co., Ltd, China (770PF, an average size d=75 μm, glass transition temperature T_g=147 ℃, melting temperature T_m=343 ℃, density ρ=1.3 g/cm^3). Molybdenum disulfide (MoS_2) nanopowders was commercially purchased

from Shanghai Yao Tian Nano Material Co., Ltd, China (≥99%, an average size d=200 nm, density ρ=5.06 g/cm^3). Graphene oxide (GO) were prepared following a modified Hummer's method by our research group in the Chemistry Laboratory. The detailed information of GO has been exhibited in Reference [31]. All materials were used as received without any further treatments.

2.2 Composites preparation

PEEK composites were prepared by using our lab's novel hot isostatic pressing method in which the heating and cooling stages of a production cycle take place in the same mold at a selected temperature and pressure [32]. The certain mass percentage of GO and/or MoS_2 were dispersed into PEEK by planetary ball mill with a speed of 800 r/min for 8 h at room temperature, respectively. The mixture was dried in a vacuum oven at 100 ℃ for 24 h. Subsequently, the constant weight mixture was loaded into a mould coated with a high temperature mould release agent MS-605, which was pressed utilizing a pressure of 5 MPa at room temperature for 30 min to remove gas. Next, the temperature was heated to 390±5 ℃ and remained for 10 h by electric heating furnace at a pressure of 3.5 MPa. Follow that, the temperature was cool down to room temperature under the pressure of 3.5 MPa, so the composites were obtained. The PEEK/GO composites with GO content of 0.3 wt.%, 0.5 wt.%, 0.7 wt.%, 0.9 wt.% and 1.0 wt.% were recorded as PG03, PG05, PG07, PG09 and PG1, respectively. The PEEK/MoS_2 composites, with different MoS_2 content 5.0 wt.%, 10 wt.%, 15 wt.%, 20 wt.% and 25 wt.%, were labeled as PM5, PM10, PM15, PM20 and PM25, respectively. The PEEK/GO/MoS_2 composite with 0.7 wt.% GO and 15 wt.% MoS_2 was labeled as PG07PM15. The composites were cut with the help of diamond cutter as per requirements. Dispersion of GO and MoS_2 in PEEK was observed by a scanning electron microscopy (SEM, Quanta 250 FEG, FEI, Czech Republic) equipped with energy dispersive spectrometry (EDS).

2.3 Tribological behaviours

Tribological behaviours of composites were investigated on a commercial tribological tester (HSR-2M, Zhongke Kaihua Technology Development Co., Ltd., China) in a pin-on-flat configuration under reciprocation motion. The friction face of the composites was held in continuous sliding contact with the steel counterpart, and a schematic diagram is shown in Figure 1. The upper specimen, i. e., the pin, was a 45 steel cylinder (a diameter of 3 mm, a length of 12 mm, a roughness of R_a=0.4 μm) and the lower specimen, i. e., the flat, was a composites cuboid (a length of 20 mm, a width of 15 mm, a thickness of 10 mm, a roughness of R_a=0.6 μm). All tribological experiments had duration of 20 min under a constant normal load of 150 N, with a reciprocation frequency of 10 Hz and stroke of 3 mm. It was conducted under dry sliding conditions at room temperature. The normal load and friction force were measured by the sensors simultaneously during the tribological experiment. Then the friction coefficients were calculated by computer automatically. The wear volume of composites was obtained by the measuring system of HSR-2M tribometer. Before each experiment, all steel pins and composites were ultrasonically cleaned with deionized water for 20 min at room temperature to ensure the surfaces cleanliness. The wear rate K was calculated by expression $K=\Delta V/PS$, where ΔV is the volume loss of the sample (mm^3), P is the normal load (N), S is the sliding distance (m). The experiments of each composite were carried out at least three times valid experiment to ensure a relevant statistical evaluation. The average value of friction coefficient and wear rate was presented in this work, with corresponding standard deviations. The worn surfaces of composites were inspected with SEM and their three dimensional morphologies were observed by a three dimensional ultrafine optical microscope (Leica DVM6, Germany). Before examination, the samples were ultrasonically cleaned in the deionized water bath for 20 min, and then plated with a thin gold layer.

 doi:10.20944/preprints202009.0438.v1

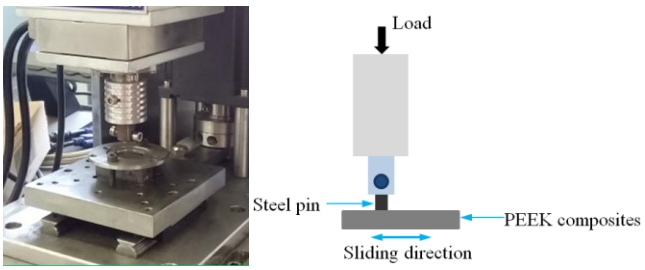

Figure 1. Schematic diagram of the pin-on-flat contact configuration of reciprocation sliding friction apparatus.

2.4 Mechanical properties

The Vickers hardness was measured on planar composite samples by a THV-5 digital Vickers microhardness tester (Beijing Time High Technology Co., Ltd., China) according to Chinese National Standard GB/T4340-2009. Before measuring, all samples surface were polished by a Masterlam polisher (Kulzer Lamplan, France), which cleaned in distilled water for 20 min by ultrasonic cleaner. A standard Vickers indenter was utilized, with a load of 1.961 N at indentation loading time of 15 s at room temperature. The indentation data were obtained by measuring system of the Vickers hardness tester. Based on load and indentation data, the Vickers hardness was calculated from expression $HV=0.1891F/d^2$, where HV is the Vickers hardness, F is the test load (N) and d is the indentation diagonal arithmetic mean value (mm). An average value of at least five random positions on each composite sample and their standard deviation were presented in this work.

Tensile test was carried out by AG-XPLUS electronic universal testing machine (Shimatsu Manufacturing Co., Ltd., Japan) according to ASTM D3039M-14 standard test method. Nominal dimensions of tensile composite were 50 mm in length, 5 mm in width and 1mm in thickness. The sample had 12 mm smooth transition from gauge to 15 mm wide shoulders. Tests were carried out at a speed 1 mm/min and at room temperature. Tensile strength was obtained by the calculating software of testing machine. At least three samples of each composite were measured to obtain the average values and standard deviation. Fractography analysis was carried out on tensile fracture surfaces, which were coated with a thin gold layer by a sputtering device to make them electric conduction. The fracture surface morphology of composite was observed by SEM in the secondary electron mode at 10 kV. Representative fracture surfaces were shown.

2.5 Thermal characterizations

Differential scanning calorimetry (DSC) tests were carried out using a Netzsch STA449F3, Germany. After 10 mg composite was pre-dried at 120 ℃ for 1 h, it was heated in an aluminum pan from room temperature up to 400 ℃ at a heating rate of 20 ℃ /min under nitrogen atmosphere. The thermal gravimetric analysis (TGA) tests were conducted by a Pyrisl Perkin-Elmer, USA. The 5 mg dried samples were loaded into ceramic pans and heated up to 800 ℃ at a heating rate of 20 ℃ /min under nitrogen atmosphere. All composite samples were measured in triplicates.

3. Results

3.1 Tribological behaviours

Friction coefficients of the situ measurements of the samples under a dry sliding condition are shown in Figure 2. It can be clearly seen that the friction coefficient of PEEK and PEEK/GOs is gradually increasing and then fluctuating in a stable range (Figure 2a). The variation of average friction coefficient gradually decreases, and then increases with increasing of the GO content.

 doi:10.20944/preprints202009.0438.v1

However, the average friction coefficient of all PEEK/GOs is lower than that of PEEK. The average friction coefficient of PEEK sample is 0.2319, suggesting PEEK has poor friction reduction capacity, which is coincide with the results of Li et al. [33]. The PG05 has an average friction coefficient of μ=0.1966, its value is only 85% that of PEEK. The PG07 has a minimum average friction coefficient of μ=0.1901, reduces 18% compared to PEEK, indicating the best friction reduction abilities. When GO content exceeds 0.7 wt.%, the average friction coefficient began to increase. For instance, PG09 has an average friction coefficient of μ=0.2171, and increases 14% than that of PG07. But the response time to a stable friction state is obviously different. The response time of PEEK is about 950 s. However, the response time of PEEK/GOs reduces with increasing of the GO content. Such as the response time of PG03 is about 500 s and reduces 47% compared to PEEK, and the values of PG05 and PG07 are about 400 s. The PG09 and PG1 decrease 63% compared with PEEK. It can be clearly found that the response time to the stable friction state decreases with the increasing of GO content. It is very important to reach stable friction state of friction pair quickly, which can greatly shorten the running-in time, reduce energy consumption and improve the performance of composites. Meanwhile，it can be observed that the friction coefficient of PEEK/MoS_2s and PEEK/GO/MoS_2 is gradually increasing at the beginning of the experiment, and then fluctuating in a stable interval with time in Figure 2b. The response time of all PEEK/MoS_2s is about 350 s and less than that of PEEK, indicating the effect of MoS_2 content on response time is very small. It can be concluded that the MoS_2 can effectively reduce the response time of PEEK/MoS_2s. For PG07PM15, the response time is around 380 s, lower than that of PG07, but higher than that of PM15, decreasing 60% compared with PEEK. The average friction coefficient of all PEEK/MoS_2s decreases with increasing of the MoS_2 content, i. e., the larger the MoS_2 content, the smaller the average friction coefficient. Such as the average friction coefficient of PM5 reduces 24% compared with PEEK. Moreover, the PM25 has a minimum average friction coefficient of μ=0.1602, which reduces 31% than that of PEEK. However, the average friction coefficient is not result in a significant change while the MoS_2 content exceeds 15 wt.%. For example, the average friction coefficient of PM15 is 0.1626, while the values of PM20 and PM25 only decrease 1.2% and 1.5% that of PM15, respectively. Furthermore, the average friction coefficient of PG07PM15 is 0.1637, which is 86% that of PG07 and 1.02 times that of PM15, respectively. This is because that the high response time and average friction coefficient of PEEK is mainly attributed to strong adhesion and plough effect on the rubbing surface, owing to its low hardness, easy plastic deformation and poor friction heat dissipation. But the friction heat loss is improved and the adhesive effect is reduced for composites. On the other hand, GO and MoS_2 play a key role of reducing friction coefficient of composites owning to their self-lubricant. The better friction reduction of PEEK/MoS_2 than PEEK/GO is attributed to the better self-lubricant of MoS_2. However, the excessive GO leads to the increase of friction coefficient. This is due to the stress concentration and increased fragility, weakening the bonding strength between GO and PEEK matrix.

Figure 2c shows the variation of wear rate of PEEK, PEEK/GOs, PEEK/MoS_2s and PEEK/GO/MoS_2. The wear rate of PEEK is 6.213×10-6 mm3/Nm, which is in the same order of magnitude with value obtained by Zhang et al. under a dry sliding condition [2]. The wear rate of PEEK/GOs significantly decreases, and then slightly fluctuates in a very small scale with increasing of GO content. When the GO content increases from 0.5 wt.% to 0.7 wt.%, the wear rate decreases obviously. However, the GO content exceeds 0.7 wt.%, the wear rate is basically constant. Regardless of the GO content, the wear rate of all PEEK/GOs is less than that of PEEK, indicating the positive effect of GO on the wear resistance. Such as the wear rate of PG03 and PG05 is 90% and 85% that of PEEK, respectively.

Preprints (www.preprints.org) | NOT PEER-REVIEWED | Posted: 18 September 2020 doi:10.20944/preprints202009.0438.v1

Nevertheless, PG07 has the lowest wear rate of K=4.169×10-6 mm3/Nm, which is 33% lower than that of PEEK. In other words, PG07 has the best wear resistance. The variation of wear rate of PEEK/MoS_2s is obvious decrease with the increasing of MoS_2 content. When the MoS_2 content is less than 20%, the wear rate of PEEK/MoS_2s approximately reduces linear, whereas the difference in wear rate between PM20 and PM25 is minimal. But, the wear resistance of PEEK/MoS_2s is significantly increased in compared with PEEK. For instance, the PM5 has the maximum wear rate of K=5.011×10-6 mm3/Nm, which is 19% lower than that of PEEK, while PM25 has the minimum wear rate of K=3.333×10-6 mm^3/Nm, reduces 46% compared with PEEK. The wear rate of PM5 is 1.5 times that of PM25. The wear rate of PG07PM15 decreased by 35% compared with PEEK, which was almost equal to that of PM15 and less than that of PG07. It can be concluded that MoS_2 plays a major role in the wear resistance of PG07PM15. It is worth to note that the abilities of friction reduction and wear resistance of the composites with both GO and MoS_2 is not necessarily better than that of the composites with single GO or MoS_2.

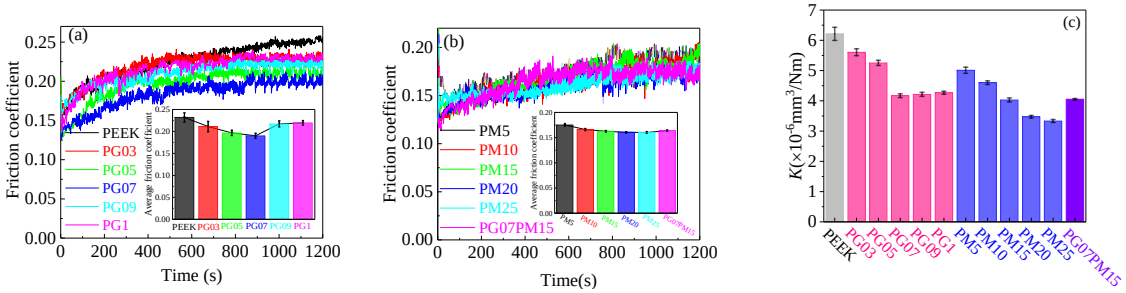

Figure 2. Friction coefficient of PEEK and PEEK/GOs (a), PEEK/MoS_2s and PEEK/GO/MoS_2 (b), wear rate of PEEK, PEEK/GOs, PEEK/MoS_2s and PEEK/GO/MoS_2 (c).

To facilitate the understanding of the mechanism of friction and wear, representative SEM images and the corresponding 3D optical morphologies of the worn surface after sliding wear tests of PEEK, PEEK/GOs, PEEK/MoS_2s and PG07PM15 are detected in Figure 3. The PEEK (Figure 3a, a') exhibits unevenly grooves parallel to the sliding direction and irregular removed material adhered back to the surface, which show signs of abrasive wear and adhesive wear mechanism. Meanwhile, there are large amount of debris on the worn surface. The typical combination mechanism of abrasive wear and adhesive wear has been previously observed under a dry sliding condition [34]. A clear boundary is produced between the worn area and non-worn area owning to PEEK stacked under the compressive load and friction force. The deep wear scratch on the surface of PEEK can be visibly seen, and the worn surface is very rough, too. The worn surface of PG03 (Figure 3b, b') is smoother than that of PEEK. Several very shallow grooves caused by abrasive wear, a typical lamellar dissection, fatigue fracture caused by cyclic load and the presence of micro-cracks, short stripped pits parallel to the sliding direction and a small amount of adhesive debris marks, indicating a certain wear characteristics of brittle materials. There is an obvious partition boundary similar with that of PEEK for PG03, PG07 and PG1. However, the height of the materials accumulation is smaller, and the wear depth of the composites is significantly smaller than that of PEEK (Figure 3c, d, c', d'). Such characteristics maybe contributed to the decrease of melting temperature of PEEK/GO. But the wear degree of the PEEK/GOs is obvious differences with content. With the increase of GO content, the fatigue wear becomes more and more dominant, and the adhesive wear and abrasive wear gradually reduce. This indicates PEEK/GOs show signs of severe fatigue wear, adhesive wear and mild abrasive wear. The PM5 (Figure 3e) represents more even grooves parallel to the sliding direction, plastic deformation, randomly adhered material and a certain amount of wear debris. Nevertheless, the worn surface of PM15 (Figure 3f) exhibits a small quantity of shallow grooves, adhered material and wear debris. Simultaneously, a water wave-like morphology is obviously observed. As same as PEEK, the worn surfaces of PM5 and PM15 result from the same wear mechanism, i. e., mainly abrasive wear and adhesive wear, just the wear degree of the individual components are different. Whereas, in the case of PM25 (Figure 3g), the worn surface shows a completely different morphological features from that of PM5 and PM15, which is very smooth and covered by an almost uniform and essentially continuous light gray layer, and that is torn signs

Preprints (www.preprints.org) | NOT PEER-REVIEWED | Posted: 18 September 2020 doi:10.20944/preprints202009.0438.v1

along the sliding direction. In addition, these gray layers can avoid direct contact between composites and the counterpart, which further improves the tribological properties of composites. It can be observed that there is very little adhesive material and plastic deformation on the worn surface, but no obvious grooves and wear debris. This indicates that PEEK/MoS_2s possesses better friction reduction and wear resistance compares to PEEK and PEEK/GOs. As shown in Figure 3e', f', g', there is still an obvious wear area boundary like all others composites. The accumulation of boundary materials is contributed to the plastic deformation of PEEK matrix. With increasing of MoS_2 content, the wear depth of worn surface reduces and the coverage rate of MoS_2 film increases, which are contribute to the unique lubrication characteristics of MoS_2. Furthermore, it is worth noted that the MoS_2 content has a positive contribution to wear resistance, i. e., the higher the MoS_2 content, the better the wear resistance (Figure 2c). The PG07PM15 (Figure 3h, h') represents very even shallow narrow grooves parallel to the sliding direction, a small quantity of micro-cracks, a water wave-like scratch, spalling pit and plastic deformation, which is smoother than that of PG07 and PM15. It can be observed that the worn surface shows neither the severe sheet spalling caused by the fatigue wear in the case PG07, nor the deep grooves and wear debris in the case PM15. Compared with other composites, a typical wear area boundary is observed in Figure 3h'. Such morphology features indicate that the wear mechanism of PG07PM15 is the combination of slight fatigue wear, mild abrasive wear and adhesive wear. It can be concluded that the synergism between GO and MoS_2 help to form a good and tenacious lubricant films on the interface between composites and counterpart.

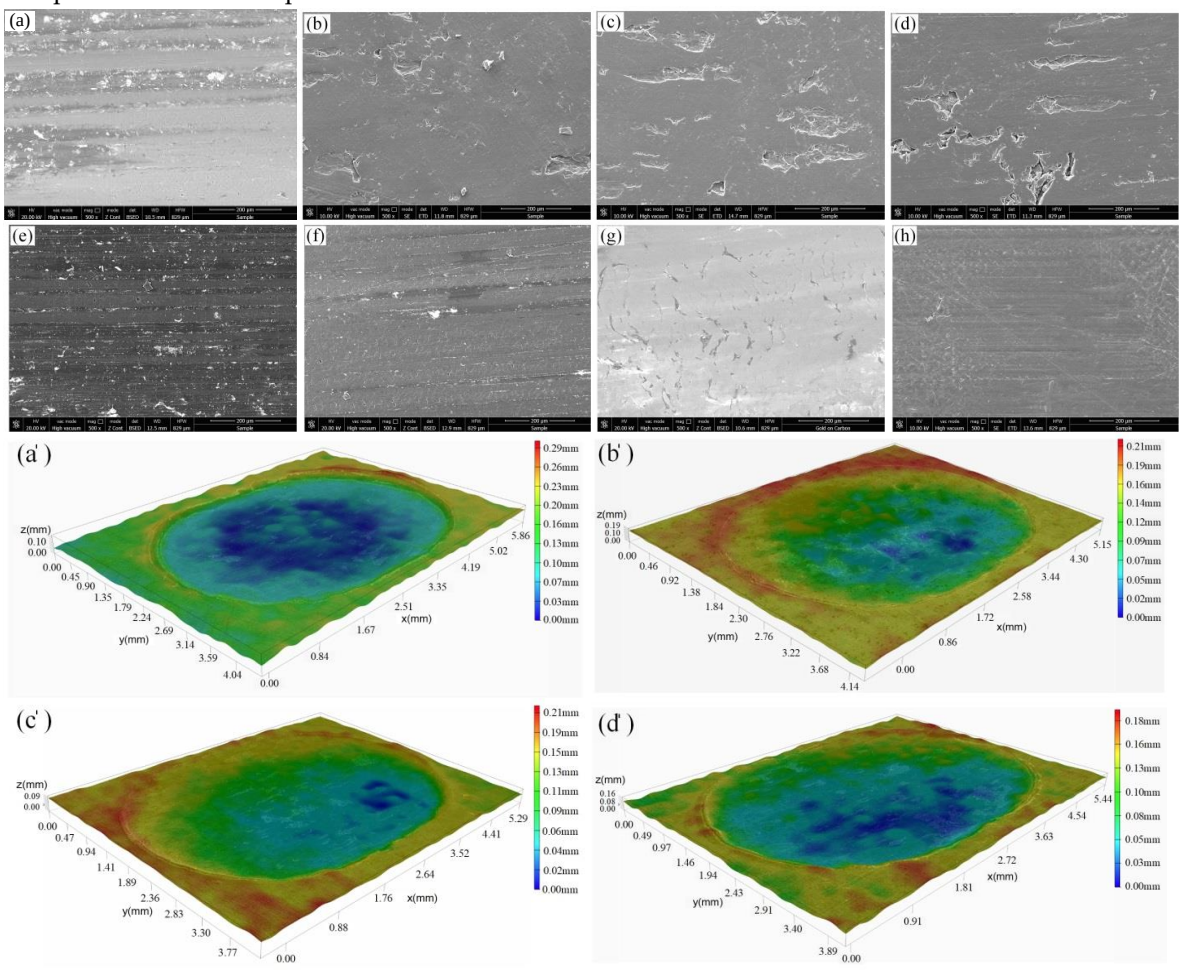

Preprints (www.preprints.org) | NOT PEER-REVIEWED | Posted: 18 September 2020 doi:10.20944/preprints202009.0438.v1

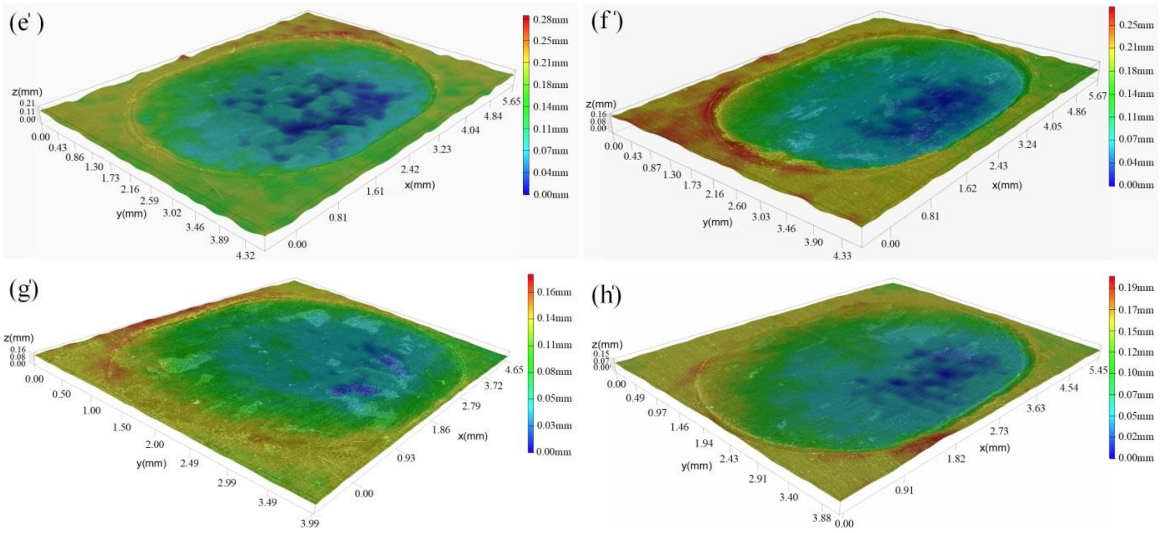

Figure 3. SEM images and 3D optical morphologies of worn surfaces. (a, a') PEEK, (b, b') PG03, (c, c') PG07, (d, d') PG1, (e, e') PM5, (f, f ') PM15, (g, g') PM25, (h, h') PG07PM15.

In order to better explain the triological properties of composites, Figure 4 presents the corresponding schematic diagram under a dry sliding condition. In the case PEEK (Figure 4a), the grooves of worn surface are mostly contributed to the stiffness of counterpart of steel pin is much higher than that of PEEK. During the friction and wear process, the hard protuberances on the steel pin penetrate into the PEEK and remove the softer PEEK under applied contact load and friction shear. On account of the combination of the plastic deformation, delamination and friction shear, the PEEK is transferred to the counterpart surface to form a lubricant film, which back to the originating PEEK surface-adhered material.

For the PEEK/GOs (Figure 4b), the wear characteristics may be the fact that the hardness and tensile strength of the composites is improved by addition of GO with large specific surface area and wrinkle, leading to less flow stress and considerably less plastic deformation for the sliding contact surface, as well as a decrease in the toughness of composites. Moreover, GO may agglomerate in the PEEK matrix, which is more likely to lead to the initiation of micro-cracks. Under the repeated stresses, the GO will be exposed gradually on the worn surface carrying most of applied load, promotes the formation of protective and in situ tribolayer in the interface between the composites and steel pin. This morphology features indicate that the addition of GO changes the main wear mechanism of composites from adhesive wear and abrasive wear to fatigue wear. The strong interface bonding of the composites made GO difficult to be detached from the PEEK matrix and effectively improved the wear resistance of the composites. However, the lubricant films on the interface will be destroyed by desquamate caused by fatigue wear as well as wear debris generated by fatigue wear. The abrasive wear is produced on the surface of composites by wear debris, which results in the shallow grooves marks. Simultaneously, the wear debris plays a certain role in grinding composites, which make its surface smooth. For PEEK/MoS_2s (Figure 4c), the MoS_2 is more easily released from the composites and exposed on the worn surface owning to the weaker bonding strength of MoS_2 and PEEK matrix. More importantly, the MoS_2 layered structure formed via weak van der Waals interactions between each layer gives better tribological performance, which makes easier to form a continuous and complete lubricant layer between the interfaces. At the same time, the softer lubricant films can effectively cover the worn surface, fill the wear marks, and make the small wear debris hidden in them. This corresponds to the better friction reduction and wear resistance of PEEK/MoS_2s in Figure 2b, c. However, for PG07PM15, GO and MoS_2 would be

Preprints (www.preprints.org) | NOT PEER-REVIEWED | Posted: 18 September 2020 doi:10.20944/preprints202009.0438.v1

concurrently exposed on the worn surface during the tribological test in Figure 4d. The GO with high mechanical strength can withstand load applied and play a certain role in lubrication, which can restrain composites being further worn off, and then the MoS_2 mostly play the lubricant effect. In a word, the lubricant films formed provides a low strength junction at the interface, resulting in lower friction coefficient and wear rate than that of PEEK. So regardless of GO or MoS_2 which are exposed to worn surface, they both can effectively avoids direct touch of the two contact surface, thus further inhibiting the wear of composites. However, the generated heat, which cannot be taken away timely or dissipated during the process of friction, will lead to the further softening of the composites and the enhancement of adhesive wear. In the meantime, the abrasive debris, difficultly discharged from the worn surface, will result in the inevitable abrasive wear under a dry sliding condition. On the contrary, the phenomenon of wear surface adhesion and a large amount of debris deposition are not almost observed due to the presence of water lubrication [3].

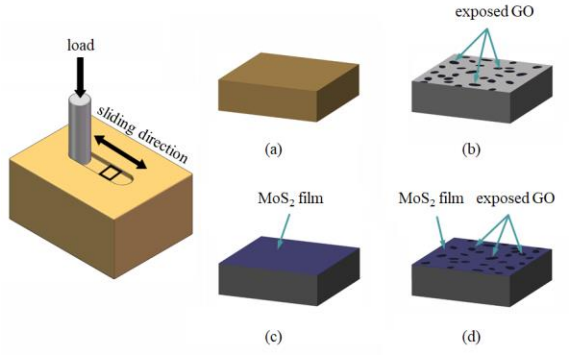

Figure 4. Schematic illustration of friction and wear of PEEK, PEEK/GOs, PEEK/MoS_2s and PEEK/GO/MoS_2.

It is well known that the nanofillers have an inherent tendency to form agglomerates due to the large surface area in the polymer matrix, and lead to decreasing of the reinforcing effects [3,11,25,35]. The homogeneity of distribution has an important effect on its hardness, tensile strength and tribological properties. In order to evaluate the dispersion of GO and MoS_2, the EDS analysis of element distribution was carried out for PG07PM15 in Figure 5. It can be clearly observed that the GO and MoS_2 were evenly dispersed in the PEEK matrix. This indicates that the hot isostatic pressing method used to prepare PEEK composites was reasonable and effective in this work, and the prepared composites could meet the experimental requirements.

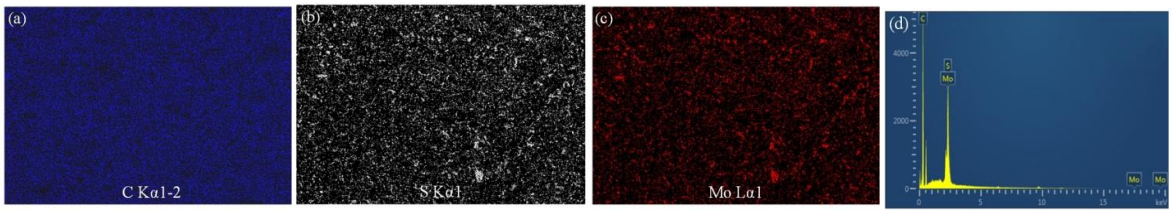

Figure 5. EDS mapping images of the PG07PM15.

3.2 Mechanical properties

The tribological properties of a material are closely related to its hardness, which is always considered to represent the scratch resistance, abrasive resistance and cutting resistance of the material surface [36,37]. To invest the reason of the super wear performance of composites, the Vickers hardness and tensile strength of PEEK, PEEK/GOs, PEEK/MoS_2s and PEEK/GO/MoS_2 are studied in Figure 6. As shown in Figure 6a, the Vickers hardness of PEEK/GOs increases with the increasing of GO content. The Vickers hardness of PG03 is 25.65 HV. And PG1 reaches to 28.39 HV,

 doi:10.20944/preprints202009.0438.v1

which is about 15% higher than that of PEEK. Interestingly, the Vickers hardness of PG07 is around 13% higher than that of PEEK, which is only 2% lower than that of PG1. This variation trend of the Vickers hardness on PEEK/GO is consistent with the reported results of Puértolas et al. [3] and Lin et al. [36]. So consideration the relationship of GO content with the Vickers hardness, the best GO content is 0.7 wt.%. It can be seen that the Vickers hardness of PEEK/MoS_2s is gradually increased firstly, and then decreased with the increasing of MoS_2 content. Simultaneously, the effect of MoS_2 on the Vickers hardness of composites is not significant. When the MoS_2 beyond 15 wt.%, the Vickers hardness decreased. The PM15 is the largest, which is 25.26 HV, and it is only 2% higher than that of PEEK. PM20 and PM25 are almost the same as PEEK. This is coincide with the results of Zalaznik et al. [25, 38]. From the standpoint of improving the Vickers hardness of PEEK/MoS_2, the optimal content of MoS_2 is 15 wt.%. The Vickers hardness of PG07PM15 is around 1.1 times that of PEEK, and it is 26.42 HV. Interestingly, its Vickers hardness is 5% higher than that of PM15, but 6% lower than that of PG07. So it confirms that GO has a better effect on improving the Vickers hardness of composites than MoS_2. The Vickers hardness enhancement of all composites could be associated to interfacial interactions between the GO/MoS_2 and the PEEK matrix, which would restrain the plastic deformation of the PEEK matrix. In addition, the addition of the GO or MoS_2 could reinforce the formation of cross-networked structures and produces the reorganization of amorphous polymer chains in the composites, in which provided a higher resistance against the normal load applied. The higher hardness of PEEK/GOs is related to the high hardness of GO [39]. The excellent hardness is benefit to the tribological properties of composites, which is coincide with the results of Figure 2.

In generally, the tensile strength of a material has close relationship with its tribological behavior [2,3]. As shown in Figure 6b. The tensile strength of PEEK is 108.3 MPa, which is in agreement with Yang et al. [40]. The tensile strength of PEEK/GOs increases with the increasing of GO content. The variation of tensile strength is approximately linearly under the GO content of 0.7 wt.%. After that, the increment of tensile strength begins to decrease. The tensile strength of PG07 is 6 % higher than that of PEEK, while PG1 is only 0.5% higher than that of PG07. Moreover, the introduction of GO could drastically affect the toughness of the composites. The contribution of GO to the improvement of tensile strength is due to GO has good compatibility with PEEK and strong binding force, improves the crystallinity and uniformity of PEEK matrix. However, when the GO content exceeds 0.7 wt.%, the tensile strength of the PEEK/GOs increases very little due to the stress concentration caused by GO agglomeration. The tensile strength of PEEK/MoS_2s increases firstly, and then decreases with the increasing of MoS_2 content. The tensile strength of PM10 is 111.1 MPa and it is 3% higher than that of PEEK. Interestingly, when the MoS_2 content exceeds 15 wt.%, the tensile strength of PEEK/MoS_2 is lower than that of PEEK. Such as the tensile strength of PM25 is only 88% of that of PEEK. It is worth note that the MoS_2 has positive effect on increment of the tensile strength of composites, but the excessive content will have negative effect. The lamellar structure of MoS_2 causes shear slip of the composites under stress. The tensile strength of PG07PM15 is smaller than that of PG07, and higher than that of PEEK and PM15, its value reaches to 112.8 MPa, which is coincide with the results of hardness. As stated above, the GO is superior to MoS_2 to improvement of tensile strength of the PEEK matrix, which is coincide with the results of Mittal et al. [41] and Puértolas et al. [3].

 doi:10.20944/preprints202009.0438.v1

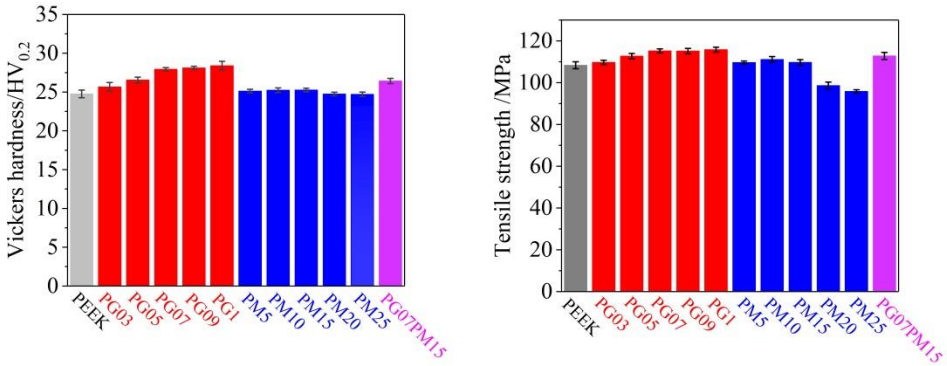

Figure 6. (a) Vickers hardness and (b) tensile strength of the different PEEK, PEEK/GOs, PEEK/MoS_2s and PEEK/GO/MoS_2.

In order to investigate the fracture properties of the composite, SEM images of fracture surface of the PEEK, PG07, PM15 and PG07PM15 after the tensile test are shown in Figure 7. The fracture surface of PEEK (Figure 7a) exhibits a relative smooth river and tongue patterns, in which appears ravines and penetrating cracks, but there is no obvious fracture dimple, fracture gully and tearing shape, reflecting that PEEK is a typical brittle fracture mode due to high strain rate, and its tensile resistance is likely the fiber cracking and pill-out. For PG07 (Figure 7b), the fracture surface shows a relatively rough squamous-like morphology with cellular on account of its brittleness, which is consistent with the decrease in toughness. The GO have good compatibility with PEEK matrix interface, which would cause crack deflection and disproportionation, could absorb tensile fracture energy and hinder the crack propagation. Therefore, the tensile strength of PEEK/GO can be improved. In case of PM15 (Figure 7c), the fracture surface exhibits a rougher morphology with wrinkle and a large amount of sheet faults in comparison with the PEEK, which indicates more effective reinforcement of the toughness. The MoS_2 are embedded in PEEK in its original layered structure, which is more likely to cause interlaminar slippage of the PEEK/MoS_2. Meanwhile, the addition of MoS_2 would destroy the continuity of PEEK, and there are many microcracks around it, in which promote the crack initiation and crack propagation. It is coincide with the tensile strength of PEEK/MoS_2. As shown in Figure 7d, the fracture surface of the PG07PM15 shows a relative rougher morphology in comparison with PEEK, exhibiting a different feature in compared with PG07 and PM15, which indicates that the presence of GO and MoS_2 can dissipate much energy and hinder the crack propagation during the fracture process. It can be observed that there are wrinkle, stacked GO sheets, microvoids and microcracks on the fracture surface. However, the obvious agglomeration phenomenon is not observed on the fracture surface, indicating a homogeneous dispersion of GO/MoS_2 in the PEEK matrix. This is coincide with the results of Vickers hardness and tensile strength.

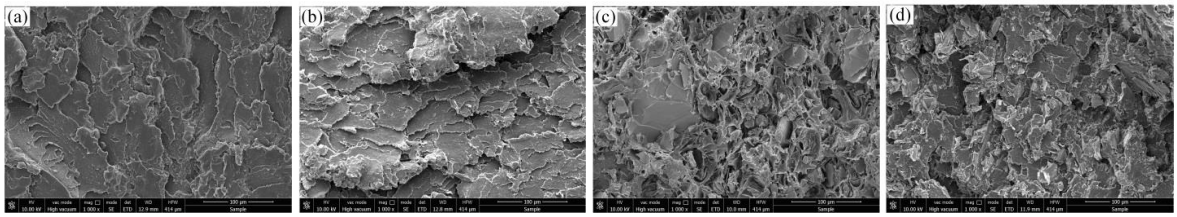

Figure 7. SEM images of fracture surfaces (a) PEEK, (b) PG07, (c) PM15, and (d) PG07PM15.

3.3 Thermal properties

In order to further understand the super tribological performance of composites, the thermal behaviours are estimate. Figure 8 illustrates the DSC and TGA curves of PEEK, PEEK/GOs and

Preprints (www.preprints.org) | NOT PEER-REVIEWED | Posted: 18 September 2020 doi:10.20944/preprints202009.0438.v1

PEEK/MoS_2s. As shown in Figure 8a, it can be observed that the melting temperature of PEEK, PG03, PG05, PG07, PG09 and PG1 is about 348.9 ℃, 348.9 ℃, 343.9 ℃, 343.9 ℃, 343.9 ℃ and 343.9 ℃, respectively. The decrease of melting temperature of PEEK/GO is contributed to the GO. When the GO content exceeds 0.5 wt.%, the melting temperature is basically constant and is 5 ℃ lower than that of PEEK. This is coinciding with the results of Puértolas et al. [3]. Interestingly, the melting temperature of all PEEK/MoS_2s is almost the same, its value is around 343.9 ℃, and lower than that of PEEK in the Figure 8b. It is coincide with the results reported by Zalaznik et al [25]. It is worth note that the MoS_2 content has no significant effect on the melting temperature. The reason is because the addition of MoS_2 or GO destroys the continuity of PEEK matrix, and the motion of the polymer chain is segmented during crystallization, in which inhibits molecular stacking, results in the formation of less perfect crystallites. As shown in Figure 8c, the PEEK/GOs exhibit a similar thermal decomposition process with PEEK, which can be mainly ascribed to the decomposition of PEEK polymer molecular chains. The onset decomposition temperature of PEEK/GOs increases with the increasing of GO content. The onset decomposition temperature and weight residue of PEEK are approximately 578 ℃ and 56%, respectively. Compared to PEEK, for lower GO content, i.e. PG03 and PG05, the thermal decomposition temperature improves 5 ℃, while that of PG07, PG09 and PG1 improves about 10 ℃. In consequence, it can be seen that GO can effectively increase the thermal stability of composites, and PEEK/GOs have higher thermal stability with increasing GO content. It is observed that PEEK/MoS_2s exhibit a different thermal decomposition process to the PEEK (Figure 8d), which can be ascribed to the barrier effect of MoS_2 on the diffusion of PEEK. The decomposition temperature of PM5 and PM10 is approximately 603 ℃. Nevertheless, the decomposition temperature of composites reaches to 608 ℃, when the MoS_2 content exceeds 15 wt.%. The decomposition temperature is higher than that of PEEK by about 25-30 ℃. It indicates that the presence of MoS_2 can effectively enhance the thermal stability of PEEK matrix. However, the weight residue of PM5, PM10, PM15, PM20 and PM25 is 74%, 74%, 76%, 77% and 79%, respectively. Compared with the PEEK, the weight residue increases 32~41%. The similar observations were reported by Chen et al. [12] and Gong et al. [42]. Therefore, it can be seen that the MoS_2 can obviously promote the thermal stability of composites. Furthermore, it can be worth note that the effect of MoS_2 on the thermal stability of composites is better than that of GO. This is mainly attributed to the MoS_2 excellent high temperature resistance and the interaction between PEEK matrix, which results in the formation of a stable network structure within the composites, preventing the PEEK chain segments from decomposition at high temperature [7,43]. In addition, the charring effect of MoS_2 at high temperature also contributes to the thermal stability of composites. As is well known, a large amount of heat will be generated during the process of friction and wear, especially under dry friction conditions [44]. It will lead to excessive degradation of the polymer and poor tribological properties. Therefore, the excellent thermal stability of composites effectively prevents the high temperature harm, and improves their tribological performances in dry sliding friction and wear conditions.

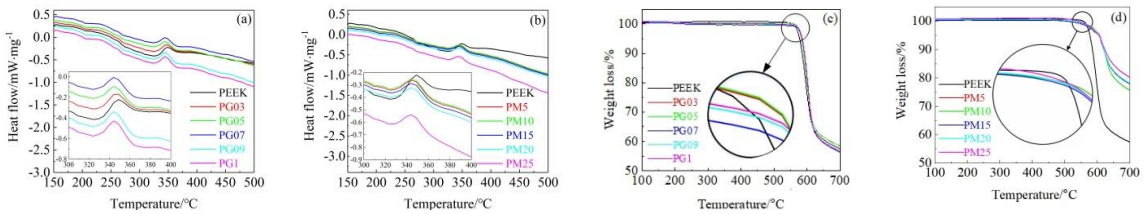

 doi:10.20944/preprints202009.0438.v1

Figure 8. DSC and TGA curves. (a, b) PEEK and PEEK/GOs and (c, d) of the PEEK and PEEK/MoS2s.

5. Conclusions

In this study, PEEK/GO and PEEK/MoS_2 composites have successfully prepared via a novel hot isostatic press method. The mapping-mode EDS exhibits that the GO and MoS_2 are evenly distributed in the PEEK matrix. The wear rate of PEEK/GOs, PEEK/MoS_2s and PEEK/GO/MoS_2 obviously reduces owing to the addition of GO and MoS_2. The response time to stable friction state reduces in compared to PEEK matrix due to the addition of GO and MoS_2 and it obviously decreases with increasing of the GO content. In addition, the addition of GO and MoS_2 effectively decreases the friction coefficient of PEEK matrix. PEEK exhibits typical combination of abrasive wear and adhesive wear mechanism. The severe fatigue wear, light adhesive wear and mild abrasive wear mechanism are found for PEEK/GO, and the fatigue wear severity increased with the increase of GO content. However, the PEEK/MoS_2 shows the abrasive wear and little adhesive wear mechanism, and it was related to the MoS_2 content. The wear mechanism of GO/PEEK/MoS_2 is mostly slight fatigue wear, mild abrasive wear and adhesive wear. The good wear resistance and friction reduction of composites are attribute to the enhancement of its hardness, tensile strength and thermal stability after the addition of GO and MoS_2.

Author Contributions: Conceptualization, Yutao Yan.; and Yuqiu. Huo.; methodology, Yutao.Yan.; investigation, Yutao Yan; Cheng Jiang; Chaofeng Li; writing—original draft preparation, Yutao.Yan.; writing—review and editing, Yutao.Yan.; Yuqiu Huo; funding acquisition, Yutao.Yan. All authors have read and agreed to the published version of the manuscript.

Funding: This research was funded by National Natural Science Foundation of China, grant number 51875095.

Conflicts of Interest: The authors declare no conflict of interest.

References

1. D. Kumar, T. Rajmohan, S. Venkatachalapathi. Wear behavior of PEEK matrix composites: a review, Materials Today Proceedings, 2018, 5(6): 14583-14589.
2. Z. Zhang, C. Breidt, L. Chang, K. Friedrich. Wear of PEEK composites related to their mechanical performances, Tribology International, 2004, 37(3): 271-277.
3. J. A. Puértolas, M. Castro, J. A. Morris, R. Ríos, A. Ansón-Casaos. Tribological and mechanical properties of graphene nanoplatelet/PEEK composites, Carbon, 2019, 141: 107-122.
4. M. S. Jahan, B. M. Walters, T. Riahinasab, R. Gnawali, D. Adhikari, H. Trieu. A comparative study of radiation effects in medical-grade polymers: UHMWPE, PCU and PEEK, Radiation Physics and Chemistry, 2016, 118: 96-101.
5. J. J. Zhu, L. Ma, R. Dwyer-Joyce. Friction and wear behaviours of self-lubricating peek composites for articulating pin joints, Tribology International, 2020, 149: 105741.
6. H. J. Song, N. Li, Y. J. Li, C. Y. Min, Z. Wang. Preparation and tribological properties of graphene/poly(ether ether ketone) nanocomposites, Journal of Materials Science, 2012, 47: 6436-6443.
7. Z. Y. Chen, H. X. Yan, T. Y. Liu, S. Niu. Nanosheets of MoS2 and reduced graphene oxide as hybrid fillers improved the mechanical and tribological properties of bismaleimide composites, Composites Science and Technology, 2016, 125: 47-54.
8. M. Sharma, J. Bijwe, P. Mitschang. Wear performance of PEEK-carbon fabric composites with strengthened fiber-matrix interface, Wear, 2011, 271(9-10): 2261-2268.
9. A. Tewatia, J. Hendrix, Z. Z. Dong, M. Taghon, S. Tse, G. Chiu, W. E. Mayo, B. Kear, T. Nosker, J. Lynch. Characterization of melt-blended graphene-poly(ether ether ketone) nanocomposite, Materials Science and Engineering: B, 2017, 216: 41-49.
10. Z. S. Cao, L. Qiu, Y. Z. Yang, Y. K. Chen, X. G. Liu. The surface modifications of multi-walled carbon nanotubes for multi-walled carbon nanotube/poly(ether ether ketone) composites, Applied Surface Science, 2015, 353: 873-881.
11. M. C. Kuo, C. M. Tsai, J. C. Huang, M. Chen. PEEK composites reinforced by nano-sized SiO_2 and Al_2O_3 particulates, Materials Chemistry and Physics, 2005, 90(1): 185-195.

12. B. B. Chen, X. Li, Y. H. Jia, X. F. Li, J. Yang, F. Y. Yan, C. S. Li. MoS_2 nanosheets-decorated carbon fiber hybrid for improving the friction and wear properties of polyimide composite, Composites Part A: Applied Science and Manufacturing, 2018, 109: 232-238.
13. M. Rinaldi, D. Puglia, F. Dominici, V. Cherubini, L. Torre, F. Nanni. Melt processing and mechanical property characterization of high-performance poly(ether ether ketone)-carbon nanotube composite, Polymer International, 2017, 66(12): 1731-1736.
14. Z. Wahab, Z. M. Marsh, A. Tessema, A. Kidane, M. Stefik, B. L. Anneaux, H. J. Ploehn. Effect of nanodiamond (ND) surface functionalization on the properties of ND/PEEK composites, IEEE Transactions on Components Packaging and Manufacturing Technology, 2017, 7(2): 165-177.
15. K. S. Novoselov, A. K. Geim, S. V. Morozov, D. Jiang, Y. Zhang, S. V. Dubonos, I. V. Grigorieva, A. A. Firsov. Electric field effect in atomically thin carbon films, Science, 2004, 306(5696): 666-669.
16. I. Clavería, D. Elduque, A. Lostalé, Á. Fernández, P. Castell, C. Javierre. Analysis of self-lubrication enhancement via PA66 strategies: texturing and nano-reinforcement with ZrO_2 and graphene, Tribology International, 2019, 131: 332-342.
17. F. Wang, H. Y. Wang, J. Mao. Aligned-graphene composites: a review, Journal of Materials Science, 2019, 54: 36-61.
18. S. H. Yetgin. Tribological properties of compatabilizer and graphene oxide-filled polypropylene nanocomposites, Bulletin of Materials Science, 2020, 43(1): 89.
19. A. Roy, L. W. Mu, Y. J. Shi. Tribological properties of polyimide-graphene composite coatings at elevated temperatures, Progress in Organic Coatings, 2020, 142: 105602.
20. S. S. Kandanur, M. A. Rafiee, F. Yavari, M. Schrameyer, Z. Z. Yu, T. A. Blanchet, N. Koratkar. Suppression of wear in graphene polymer composites, Carbon, 2012, 50(9): 3178-3183.
21. B. L. Pan, J. Zhao, Y. Q. Zhang, Y. Z. Zhang. Wear performance and mechanisms of polyphenylene sulfide/polytetrafluoroethylene wax composite coatings reinforced by graphene, Journal of Macromolecular Science, Part B-Physics, 2012, 51(6): 1218-1227.
22. N. Agrawal, A. S. Parihar, J. P. Singh, T. H. Goswami, D. N. Tripathi. Efficient nanocomposite formation of acrylo nitrile rubber by incorporation of graphite and graphene layers: reduction in friction and wear rate, Procedia Materials Science, 2015, 10: 139-148.
23. R. B. Surya, S. Balaji, A. N. A. B. Mohamed. Tribological performance of graphene/graphite filled phenolic composites-a comparative study, Composites Communications, 2019, 15: 34-39.
24. A. Chih, A. Ansón-Casaos, J. A. Puértolas. Frictional and mechanical behaviour of graphene/UHMWPE composite coatings, Tribology International, 2017, 116: 295-302.
25. M. Zalaznik, S. Novak, M. Huskić, M. Kalin. Tribological behaviour of a PEEK polymer containing solid MoS_2 lubricants, Lubrication Science, 2016, 28(1): 27-42.
26. H. X. Wu, S. C. Yin, Y. Du, L. P. Wang, H. F. Wang. An investigation on the lubrication effectiveness of MoS2 and BN layered materials as oil additives using block-on-ring tests, Tribology International, 2020, 151: 106516.
27. V. Bhardwaj, R. K. Pandeyb, V. K. Agarwal. Experimental investigations for tribo-dynamic behaviours of conventional and textured races ball bearings using fresh and MoS_2 blended greases, Tribology International, 2017, 113: 149-168.
28. M. R. Yi, C. H. Zhang. The synthesis of MoS_2 particles with different morphologies for tribological applications, Tribology International, 2017, 116: 285-294.
29. G. G. Tang, J. Zhang, C. C. Liu, D. Zhang, Y. Q. Wang, H. Tang, C. S. Li. Synthesis and tribological properties of flower-like MoS_2 microspheres, Ceramics International, 2014, 40(8): 11575-11580.
30. K. H. Hu, X. G. Hu, J. Wang, Y. F. Xu, C. L. Han. Tribological properties of MoS_2 with different morphologies in high-density polyethylene, Tribology Letters, 2012, 47(1): 79-90.
31. S. B. Zhang, Y. T. Yan, Y. Q. Huo, Y. Yang, J. L. Feng, Y. F. Chen. Electrochemically reduced graphene oxide and its capacitance performance, Materials Chemistry and Physics, 2014, 148(3): 903-908.
32. Y. T. Yan, C. F. Li, D. Wang, Y. Li, T. L. Zhang. A novel hot isostatic pressing device, Chinese Patent, 2019, ZL201810031099. X.
33. E. Z. Li, W. L. Guo, H. D. Wang, B. S. Xu, X. T. Liu. Research on tribological behavior of PEEK and glass fiber reinforced PEEK composite, Physics Procedia, 2013, 50: 453-460.
34. M. Kalin, M. Zalaznik, S. Novak. Wear and friction behaviour of poly-ether-ether-ketone (PEEK) filled with graphene, WS_2 and CNT nanoparticles, Wear, 2015, 332-333: 855-862.

35. S. Chatterjee, F. Nafezarefi, N. H. Tai, L. Schlagenhauf, F. A. Nüesch, B. T. T. Chu. Size and synergy effects of nanofiller hybrids including graphene nanoplatelets and carbon nanotubes in mechanical properties of epoxy composites, Carbon, 2012, 50(15): 5380-5386.
36. Q. L. Lin, L. J. Qu, Q. F. Lü, C. Q. Fang. Preparation and properties of grapheme oxide nanosheets/cyanate ester resin composites, Polymer Testing, 2013, 32(2): 330-337.
37. Q. L. Lin, R. G. Zheng, P. H. Tian. Preparation and characterization of BMI resin/graphite oxide nanocomposites, Polymer Testing, 2010, 29(5): 537-543.
38. M. Zalaznik, M. Kalin, S. Novak, G. Jakša. Effect of the type, size and concentration of solid lubricants on the tribological properties of the polymer PEEK, Wear, 2016, 364-365: 31-39.
39. X. R. Zhang, X. Q. Pei, Q. H. Wang. Friction and wear studies of polyimide composites filled with short carbon fibers and graphite and micro SiO_2, Materials and Design, 2009, 30(10): 4414-4420.
40. L. L. Yang, S. L. Zhang, Z. Chen, Y. L. Guo, J. S. Luan, Z. Geng, G. B. Wang. Design and preparation of graphene/poly(ether ether ketone) composites with excellent electrical conductivity, Journal of Materials Science, 2014, 49(5): 2372-2382.
41. V. Mittal, A. U. Chaudhry. Polymer-graphene nanocomposites: effect of polymer matrix and filler amount on properties, Macromolecular Materials and Engineering, 2015, 300(5): 510-521.
42. K. L. Gong, X. H. Wu, G. Q. Zhao, X. B. Wang. Nanosized MoS_2 deposited on graphene as lubricant additive in polyalkylene glycol for steel/steel contact at elevated temperature, Tribology International, 2017, 110: 1-7.
43. Y. H. Lai, M. C. Kuo, J. C. Huang, M. Chen. On the PEEK composites reinforced by surface-modified nano-silica, Materials Science and Engineering A, 2007, 458(1-2): 158-169.
44. B. B. Chen, X. Li, Y. H. Jia, L. Xu, H. Y. Liang, X. F. Li, J. Yang, C. S. Li, F. Y. Yan. Fabrication of ternary hybrid of carbon nanotubes/graphene oxide/MoS_2 and its enhancement on the tribological properties of epoxy composite coatings, Composites Part A: Applied Science and Manufacturing, 2018, 115: 157-165.